Fundamental Investigations on the Incremental Forming of Nonwoven-Reinforced Organo Sheets

D. Nettig[1], J.-E. Rath[2], and T. Schüppstuhl[3]

[123]Institute of Aircraft Production Technology, Hamburg University of Technology, Denickestr. 17, 21073 Hamburg, Germany
[1]Email: doran.nettig@tuhh.de, Web Page: https://www.tuhh.de/ifpt/
[2]Email: jan-erik.rath@tuhh.de, Web Page: https://www.tuhh.de/ifpt/
[3]Email: schueppstuhl@tuhh.de, Web Page: https://www.tuhh.de/ifpt/

Keywords: Incremental sheet forming, Fiber reinforced plastic, Recycling

Abstract
Nonwoven fibre-reinforced thermoplastics (nw-FRTP) are traditionally thermoformed in processes requiring costly moulds. A more flexible approach suitable for prototype and small-batch production could be incremental sheet forming (ISF). While ISF of metal sheets has long been a subject of research, nonwoven reinforced organo sheets have not been investigated yet. Therefore, this study uses an incremental punch test to examine the fundamental characteristics of nw-FRTP in incremental forming. A robot-guided tool with a hemispherical tip and localisable heating are employed to deform a nonwoven recycled carbon fibre (nw-rCF) reinforced organo sheet. Supplementary material investigations are carried out to understand the observed effects. Results indicate successful localization of heating and deformation. Despite challenges such as temperature gradients and material deconsolidation, the experiments demonstrate promising potential for the incremental forming of nonwoven organo sheets.

1. Introduction

Fibre-reinforced plastics (FRP) represent a steadily growing market segment [1]. Their high specific stiffness and strength make them especially well-suited for lightweight applications. The use of a thermoplastic matrix enables new manufacturing, integration, and joining strategies that are not possible with classic thermosets [2], [3]. Furthermore, fibre-reinforced thermoplastic (FRTP) parts offer significantly higher recycling potential [4]. In the field of FRTP, so-called organo sheets, a unique type of pre-impregnated and pre-consolidated flat semi-finished product, are commonly used.

When it comes to mechanical performance, continuous fibre reinforcements are unmatched. However, in terms of recyclability and resource efficiency, nonwovens, in particular, hold immense promise as a reinforcing material in organo sheets. The recovery of fibre reinforcements often leads to a substantial reduction in fibre length [4]. In contrast, nonwovens can be directly produced from recycled staple fibres [5]. The development of processes for the production of nonwovens with high preferential orientation could further enhance the mechanical performance of nonwoven-reinforced FRPs, a direction that current research efforts are focusing on [6].

Parts production from organo sheets is usually realized in the thermoforming process using complex and expensive moulds [3]. However, a more flexible alternative for prototype and small-batch production would be desirable. The problem of long lead times and high investment costs resulting from mould-making applies not only to the forming of organo sheets but also to classic sheet metal. In order to address this issue, investigations into alternative, more flexible processes have been undertaken since the 1960s [7]–

[10]. Unlike many alternatives, the incremental forming process has been the subject of extensive research, particularly over the last twenty-five years [11]. In recent years, incremental sheet metal forming has even been commercialised [12], [13].
The basic idea of incremental forming has remained mostly unchanged: A geometrically simply shaped tool that is small relative to the material sheet produces the desired geometry through consecutive local deformations. Although in the past, incremental forming was used primarily for the forming of metal sheets, its applicability to various thermoplastics has also been demonstrated and investigated [14]. In recent years, some initial work has also been carried out on the incremental forming of short and continuous fibre-reinforced organo sheets [11], [15]–[20]. However, to the authors' knowledge, the incremental forming of nonwoven-reinforced organo sheets has not yet been investigated.
Therefore, the aim of this work is to gain fundamental insights into the behaviour of organo sheets with nonwoven reinforcement in the context of incremental forming. A punch test setup is developed and employed, described in section 2. . Supplementary experiments are performed to improve the understanding of the observed effects. First, insights are gained into the heating and forming behaviour, the failure mechanisms, and the unique challenges of the investigated material in the context of incremental forming. Significant differences are found in comparison to the behaviour of short and continuous fibre-reinforced thermoplastics.

2. Materials and Methods

2. 1. Materials

FRPs allow for a wide range of material combinations. As mentioned in section 1. , this work focuses on nonwoven reinforced organo sheets. Inorganic fibres are by far the most relevant in the composite market [1]. From an economic point of view, the recycling of carbon fibres is more sensible because of their higher production cost [21]. Therefore, the material investigated in this study is a nonwoven recycled carbon fibre-reinforced polyamide-6 (nw-rCF-PA6). The sheets used in this work have a fibre volume fraction of 30% and a thickness of approx. 1 mm.

2. 2. Main Experimental Setup

The concept of the main experimental setup is that of a heat-assisted punch test, similar to Okada et al. [15]. A rectangular sample is clamped along a circular edge. It is locally heated from both sides, with the heating applied in the centre of the sample and orthogonal to its surface. After the target temperature is reached, the sample is formed with a small hemispherical punch that performs a uniaxial, reciprocating motion. The temperature on the bottom side of the sample is measured, and the axial forming force and tool displacement are recorded.
The experimental setup is shown in Figure 1. The sample holder (b7) is fixed on top of an aluminium profile assembly. It is equipped with a rectangular pocket to allow the insertion of quadratic samples with an edge length of 100 mm. The holder also features a circular cutout with a diameter of 70 mm below the sample. Above the holder is the clamping assembly, which consists of several components, including the stamp (a6) with a ring-shaped shoulder. This shoulder with an inner diameter of 70 mm, together with the cutout in the holder, results in the samples being clamped along a circular edge. Therefore, the free surface of the sample is a disc with a diameter of 70 mm. To clamp the specimens, the stamp is activated via linearely guided tie rods (b5) that are actuated by a pneumatic cylinder with a clamping force of 785 N. The tool (a1) consists of a cylinder with exchangeable hemispherical tips of 5 to 15 mm diameter. This punch is connected to an ATI 65 load cell, which in turn is connected to the six-axis KUKA KR300 R9000 robot used to guide the movement of the tool. For the tool movement, a constant downward movement is superimposed with a reciprocating movement. The resulting motion is one in which the tool iteratively moves to a target depth, which increments with a step size of 0.2 mm. After reaching the current target depth it retracts a constant distance of 0.875 mm and moves down again to the next target depth. The movement speed is set to 1.75 mm s^{-1}.

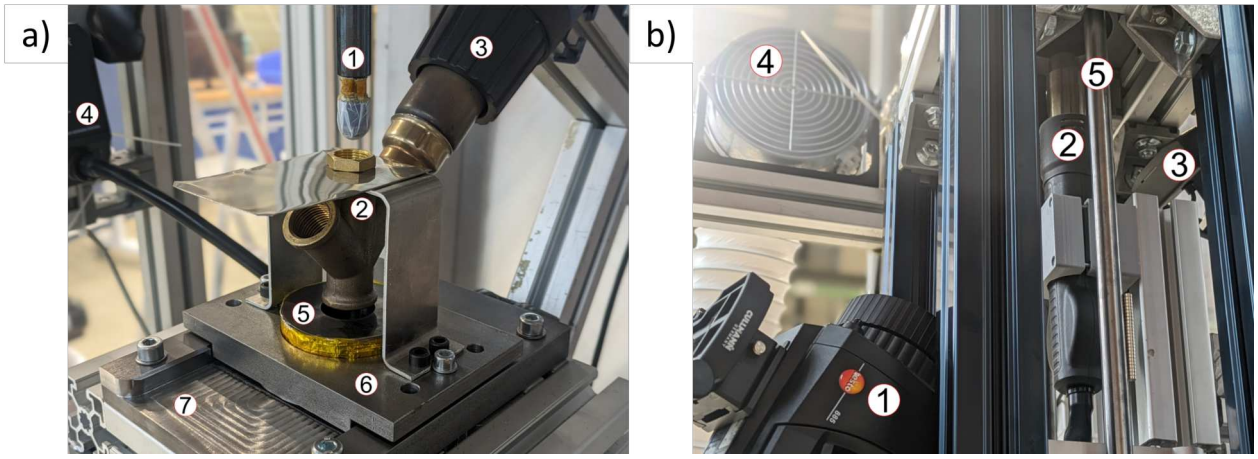

Figure 1: Experimental setup a) top view b) bottom view

A hot air blower assembly (a3) enables the heating of the sample coaxially to the punch. Another hot air blower (b2) with its controller (a4) on the opposite side of the sample allows for double-sided heating. The localisation of the heating can be enhanced by a sheet metal sleeve with insulation material (a5), which concentrates the airflow of the top blower to a circular surface of 30 mm in diameter. Conversely, placing similar insulation with air channels around its circumference slightly lifted above the sample is used to enable a more global heating. In the following, the first configuration will be called 'local' heating, while the latter will be referred to as 'global'. A ventilation system (b4) is used to remove potential evaporates. An RGB camera (b3) and a thermal imaging camera (b1) below the sample record the heating and forming procedure.

2. 3. Supplementary Investigations

Supplementary investigations were performed to better understand the heating behaviour and support the interpretation of the main experimental results. For the heating behaviour, a thermogravimetric analysis (TGA) is carried out on two samples.
To investigate the resulting deformed sample geometry, digital and physical cross sections are examined. Several samples are digitized using a Shining3D EinScan-SP V2. The captured point clouds are meshed, and digital cross-sections are subsequently generated. One heated but undeformed and one deformed sample are also physically cut and viewed with a MIRAZOOM MZ902 digital microscope.

3. Results and Discussion

An essential material behaviour, potentially pivotal for this material type, is already observed during heating. After reaching a surface temperature of about 180 °C, significant deconsolidation and expansion of the sample can be seen. This effect is clearly depicted in Figure 2.
TGA results do not show significant evaporation of bound water or impurities in the temperature range around 180 °C, for which the expansion phenomenon can be observed. Therefore, it is most likely that during the production of the organo sheets, the reinforcement is heavily compressed and elastically deformed. It is then fixed in this configuration by matrix solidification. Softening of the matrix can release this fixation, allowing the reinforcement to loft and expand back to its stress-free initial configuration.
Preliminary tests demonstrated the feasibility of localised heat input, evidenced by the localised deconsolidation (Figure 2). Material expansion likely supports localisation, as expanded regions act as insulators. An analysis of the temperature distribution within the sample plane is depicted in Figure 3a. Temperatures are

Figure 2: Expanded sample (yellow material detached from the insulation)

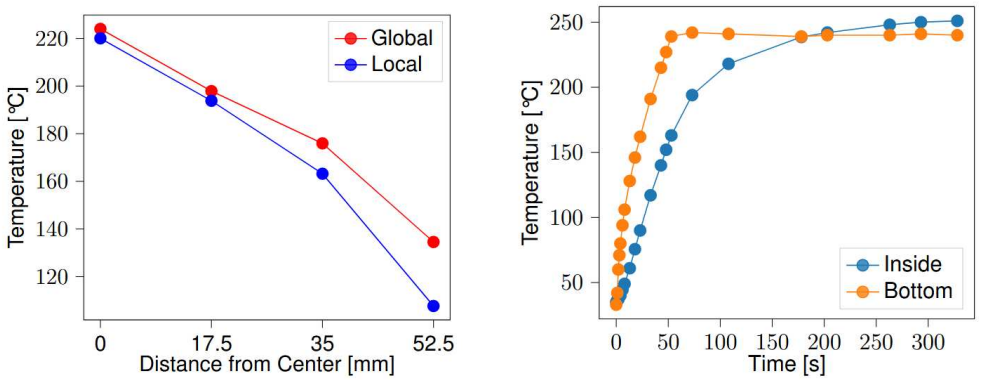

(a) In-plane temperature profile. **(b) Through-plane temperature convergence.**

Figure 3: Temperature behaviour of the samples

shown at four equally spaced (17.5 mm) points on the bottom of the sample after a five-minute double-sided heating period, for both local and global heating. While global heating seemingly leads to a slight overall temperature increase, the temperature profile in the centre is identical. From the second measurement point onward, the influence of localisation becomes apparent. In total, the difference in temperature increases from 4 °C at the centre to nearly 27 °C at the sample's edge. Thus, temperature localization within the sample remains evident even after prolonged heating.

However, the apparent low thermal conductivity also results in a substantial temperature gradient between the top and bottom surfaces. The temperature distribution perpendicular to the sample plane is illustrated in Figure 3b. Surface temperature is captured using a thermal camera, while temperature slightly below the surface is measured with a thermocouple. On the one hand, the final temperature at both positions differs only marginally, with a slightly higher inside temperature, which could be due to a slightly higher heat input of the upper blower or measurement inaccuracy. On the other hand, the time response of the temperature convergence differs significantly. Surface temperature reaches its equilibrium within approximately one minute, while it takes about 5 minutes for the internal temperature. The through-plane heat conductivity therefore seems to be low as well.

This is reflected in the heat-dependent formability as well. When only employing the upper hot air blower, plastic deformation is only achievable with airflow temperatures reaching up to 600°C. With double-sided heating, though, deformation at airflow temperatures well below the decomposition temperature of the matrix becomes possible. Higher temperatures still lead to better formability and lower forces. During the forming process, an elastic deformation of the entire sample is observed, especially for lower temperatures

Figure 4: Examples of sample failure

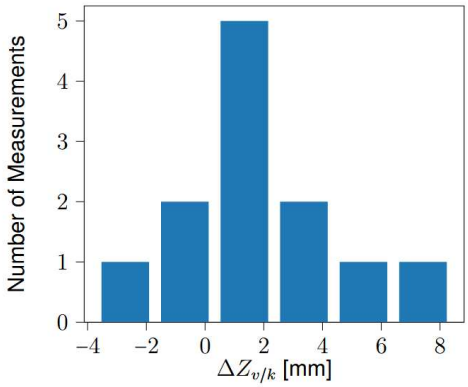

Figure 5: Incidence of differences between the point of maximum force and visually confirmed failure

and larger tool diameters. Conversely, permanent deformation occurs only locally around the punch. The remainder of the sample appears flat after tool retraction, with no observable wrinkling, cracks or indentation. Figure 4 exemplifies the visually confirmable failure after forming. Holes are observed either at the circumference of the formed cone or directly at the tip of the samples. During deformation, the formation of the holes is indicated by surface tearing before complete material failure.

Visually capturing the failure of the samples is challenging due to the surface structure of the deconsolidated samples and the gradual nature of failure. To examine the suitability of maximum force as an alternative failure criterion, the difference between the visually observable failure point and the point of maximum force is compared. For visual failure detection, the point is chosen where surface tearing is first evident.

The difference between visually observed failure depth (Z_{visu}) and failure depth measured via maximum force (Z) $\Delta Z_{v/k} = Z_{visu} - Z$ of 12 samples is depicted in Figure 5. While only visual failure detection significantly before reaching maximum force occurred only once, visual detection significantly after exceeding maximum force was more common. However, it becomes evident that visually observed failure and the point of maximum force often closely align, indicating a strong correlation between them.

The digital cross sections of three samples are depicted in Figure 6. Section a) illustrates a sample formed with a small tool diameter at a high localised temperature. A large tool diameter was used for samples b) and c), and the temperature was not localised. Sample b) was formed at a high temperature (280 °C), and sample c) at a low temperature (220 °C). The shape of the formed sample surface on the upper side corresponds to a convex cone for all samples. The resulting dome on the lower side is of a more concave shape. The forming zone on both sides is significantly larger than the tool diameter. All samples are significantly expanded throughout the heated area. Overall, the thickness decreases in the formed area towards the tip. This is particularly pronounced in sample a). For large tool diameters, especially sample c), the thickness distribution is more uniform. Also, there is a smoother transition to the expanded area at a lower temperature

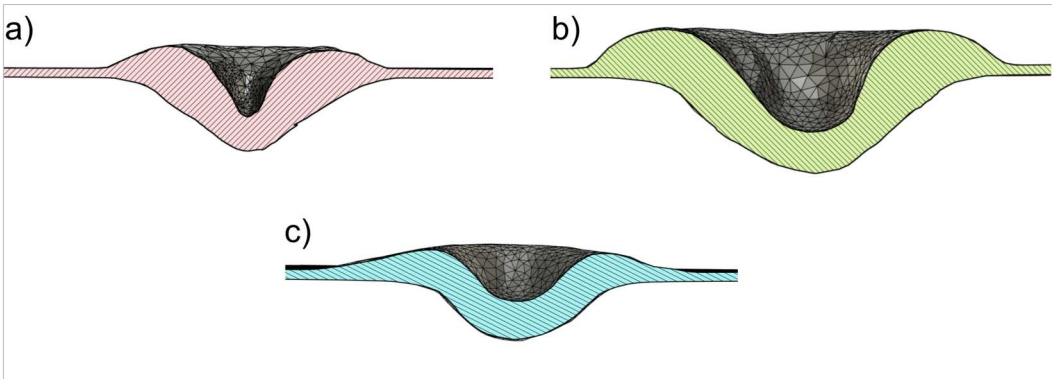

Figure 6: Digital cross sections of 3D-scanned samples

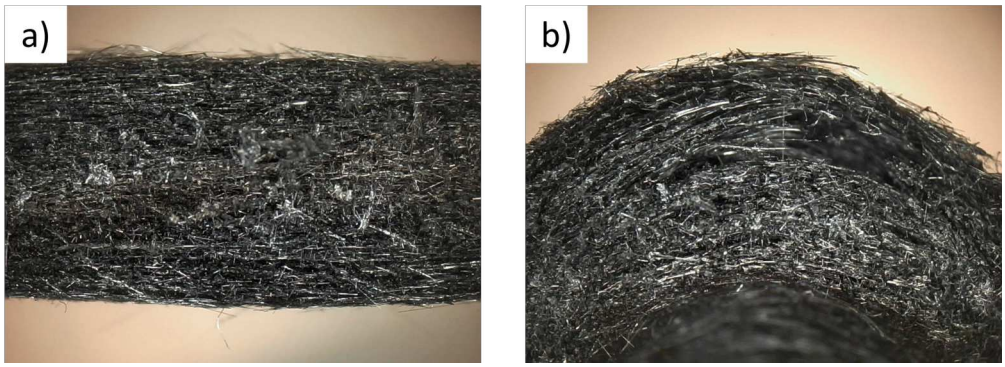

Figure 7: Sample cut surfaces a) heated but not formed b) heated and formed

(sample c)). Overall, the expansion on the upper side is less pronounced at lower temperature, but in the formed area, the thickness difference is minimal.
The microscopy images of the cut samples are shown in Figure 7. The expansion (a)) leads to a quite homogeneous cut surface. No obvious delamination, larger voids, or defects are visible. In contrast, the cut surface of the formed sample appears different. While no clear damage is visible from the outside, the cut clearly shows a significant internal defect. Just below the surface, a layer is torn over a large area, forming a cavity. At the ends of the torn layer, delamination is visible as well. Failure mechanisms can thus be identified as delamination and tearing of individual nonwoven layers. It cannot be conclusively determined whether the layer was first ripped and then detached or vice versa. Such internal failure mechanisms are a possible explanation for the difference in visual failure detection and the point of maximum force described earlier. It also implies that visual failure detection on the surface is not well suited for the material studied in this work.

4. Conclusion

In conclusion, the incremental forming characteristics of the studied nw-rCF reinforced PA6 organo sheets differ significantly from previous investigations on the incremental forming of short and continuous FRTP. Global heating, as inevitably used in ISF of continuous FRTP, is not necessarily advised. In contrast, localised heating can limit the observed deconsolidation effect and can be utilised to precisely localise the deformation. In conjunction with local heating, the nonwoven-reinforced sheets show the ability for circumferential clamping, which is not possible for continuous fibre-reinforced sheets. Furthermore, the need

for sacrificial metal sheets, often used to support globally heated organo sheets in ISF, could be avoided. Wrinkling and fibre breakage, significant issues with continuous fibres, are not observed. Compared to short fibre-reinforced organosheets, the matrix does not bleed or drip out even if its melting temperature is exceeded, due to the adhesion between the matrix and the fibre structure,
However, the incremental forming of nonwoven rCF-reinforced organo sheets also brings unique challenges, namely low heat conduction and deconsolidation. Because of the low heat conduction, a single-sided heating system might not be applicable, especially for sheets of higher thickness. Besides the development of an appropriate heating system, the most significant challenge will most likely be to find a method that avoids or reverses the expansion and deconsolidation of the sheets. Further investigations of the exact cause and magnitude of this effect will be necessary. Possible solutions could be found in material selection and preparation, the production of the semi-finished sheets, and the application of in-process pressure, e.g., by utilizing a vacuum bag or two opposing tools. When these issues are addressed, nonwoven rCF-reinforced organo sheets show promising incremental forming characteristics.

Acknowledgements
Research was funded by the German Federal Ministry for Economics and Climate Action under the Program LuFo VI-1 project iFish.

References

[1] E. Witten, V. Mathes, M. Sauer and M. Kühnel. *Composites market report 2018: Market developments, trends, outlooks and challenges*. 2018.

[2] G. Ehrenstein. *Faserverbund-Kunststoffe: Werkstoffe – Verarbeitung – Eigenschaften*. 2., völlig überarbeitete Auflage. Hanser Verlag, 2006. ISBN: 978-3-446-45754-6.

[3] M. Neitzel, P. Mitschang and U. Breuer. *Handbuch Verbundwerkstoffe: Werkstoffe, Verarbeitung, Anwendung* (Hanser eLibrary). 2., aktualisierte und erweiterte Auflage. München: Hanser, 2014. DOI: 10.3139/9783446436978.

[4] R. Bernatas, S. Dagreou, A. Despax-Ferreres and A. Barasinski. Recycling of fiber reinforced composites with a focus on thermoplastic composites. *Cleaner Engineering and Technology*. Vol. 5, pp. 100–272. 2021. DOI: 10.1016/j.clet.2021.100272.

[5] F. IGCV. *Pressemeldung nassvliesanlage: Neo-ökologie mittels innovativer papiertechnik*. 2022.

[6] Frauenhofer IGCV. *Mai scrap sero | from scrap to secondary ressources: Highly orientated wet-laid-nonwovens from cfrp-waste*. [Online]. Available: https://www.igcv.fraunhofer.de/de/forschung/referenzprojekte/mai_scrap_sero.html (visited on 09/11/2023).

[7] E. Leszak. Apparatus and process for incremental dieless forming. *United States Patent Office*. No. 3,-342,051. 1964.

[8] N. Nakajima. A newly developed technique to fabricate complicated dies and electrodes with wires. *Bulletin of JSME*. No. Volume 12, Issue 54. 1969. DOI: 10.1299/jsme1958.12.1546.

[9] S. G. Kaufman, B. L. Spletzer and T. L. Guess. Freeform fabrication of polymer-matrix composite structures. In *Proceedings of International Conference on Robotics and Automation*. 1997, pp. 317–322. DOI: 10.1109/ROBOT.1997.620057.

[10] A. K. Miller, M. Gur, A. Peled, A. Payne and E. Menzel. Die-less forming of thermoplastic- matrix, continuous-fiber composites. *Journal of Composite Materials*. Vol. 24. No. 4, pp. 346–381. 1990. DOI: 10.1177/002199839002400401.

[11] R. Conte, G. Ambrogio, D. Pulice, F. Gagliardi and L. Filice. Incremental sheet forming of a composite made of thermoplastic matrix and glass-fiber reinforcement. *Procedia Engineering*. Vol. 207, pp. 819–824. 2017. DOI: 10.1016/j.proeng.2017.10.835.

[12] Desktop Metal Inc. *Figur g15: Product brochure*. [Online]. Available: https://figur.desktopmetal.com/ (visited on 27/10/2023).

[13] Machina Labs Inc. *Home | machina labs*. [Online]. Available: https://machinalabs.ai/ (visited on 15/03/2023).

[14] G. Ambrogio, R. Conte, F. Gagliardi, L. de Napoli, L. Filice and P. Russo. A new approach for forming polymeric composite structures. *Composite Structures*. Vol. 204, pp. 445–453. 2018. DOI: 10.1016/j.compstruct.2018.07.106.

[15] M. Okada, T. Kato, M. Otsu, H. Tanaka and T. Miura. Development of optical-heating-assisted incremental forming method for cfrtp sheet - fundamental forming characteristics in spot-forming -. *Procedia Engineering*. Vol. 207, pp. 813–818. 2017. DOI: 10.1016/j.proeng.2017.10.834.

[16] A. Al-Obaidi, A. Graf, V. Kräusel and M. Trautmann. Heat supported single point incremental forming of hybrid laminates for orthopedic applications. *Procedia Manufacturing*. Vol. 29, pp. 21–27. 2019. DOI: 10.1016/j.promfg.2019.02.101.

[17] S. Torres, R. Ortega, P. Acosta and E. Calderón. Hot incremental forming of biocomposites developed from linen fibres and a thermoplastic matrix. *Strojniški vestnik – Journal of Mechanical Engineering*. Vol. 67. No. 3, pp. 123–132. 2021. DOI: 10.5545/sv-jme.2020.6936.

[18] R. Emami, M. J. Mirnia, M. Elyasi and A. Zolfaghari. An experimental investigation into single point incremental forming of glass fiber-reinforced polyamide sheet with different fiber orientations and volume fractions at elevated temperatures. *Journal of Thermoplastic Composite Materials*. 2022. DOI: 10.1177/089270572-21074266.

[19] S. Bagheri, A. Kami and M. Shakouri. Single point incremental forming of polyamide/30 wt% short glass fiber composite. *Journal of Thermoplastic Composite Materials*. Vol. 0. No. 0, pp. 1–14. 2022. DOI: 10.1177/0892705721083497.

[20] J.-E. Rath and T. Schüppstuhl. Tool path strategies for single point incremental forming of fiber-reinforced thermoplastic sheets. In *Material Forming: ESAFORM 2024*. Ser. Materials Research Proceedings. Materials Research Forum LLC, 2024, pp. 641–650. DOI: 10.21741/9781644903131-3171.

[21] W. Schade, S. Mader and M. Lembke. *Analysis of the light weight fiber reinforced plastics value chain with regard to the german industry in its global context*. Karlsruhe, 2017.